(RESEARCH ARTICLE)

Check for updates

Capillary ultrastructure anatomy and physiology: What is known, what is unknown or missing, what is wrong and what is new?

Ahmed N Ghanem *

Egypt Retired Consultant Urologist Surgeon & Independent Investigator 10 Merton Court, Faculty of Medicine, Mansoura University, The Strand, Brighton Marina, BN2 5XY. The UK.

Abstract

This article summarizes what is already known about the capillary ultrastructure anatomy and physiology that includes one wrong physiological law of Starling and two misconceptions on capillaries cross section area and blood speed in its lumen. It also identifies missing data such as the number and diameters of capillaries branching from the terminal arteriole, and the speed of blood at the arterial and venous ends. It also summaries the evidence on new knowledge on capillary physiology namely the hydrodynamic of the porous orifice (G) tube built on a scale to capillary ultrastructure anatomy of pre-capillary sphincter and inter-cellular slits pores. It proves Starling's law wrong and provide its correct replacement. The Tree Branching Law (TBL) corrects both misconceptions on capillaries cross section area being larger that the aorta and capillary blood speed is "very slow". The TBL proves that the cross-section area of all capillaries is less than that of the aorta, and the blood speed in capillary is faster than generally received. The G tube' magnetic field like hydrodynamics is the correct replacement for Starling's law on the capillary-ISF transfer. This new capillary-ISF transfer allows for fast efficient function that meets cells and tissue demands at rest and during strenuous exercise.

Keywords: Capillary physiology; Capillary blood speed and pressure; Starling's law; Hydrodynamics; The porous orifice G tube; Tree Branching Law

1. Introduction

What is known about the capillary?

The vascular capillary is the microtubule that connects an arteriole to venule. It is functionally responsible for the passage of gases and nutrients from blood into the body cells. It is exceedingly small, measuring 5-10 micrometres (μm) in diameter, only allows red blood cells (RBCs) to pass through one cell at a time. Walls are made of semi-permeable membrane to allow transport of gases and nutrients into and out of the blood.

1.1. Anatomical Structure of Capillaries [1]

Capillaries are composed of a thin layer of epithelial cells and a basal lamina, or basement membrane, known as the tunica intima. There is also an incomplete layer of cells that partially encircles the epithelial cells, known as pericytes. Microvascular pericytes regulate blood pressure in the capillaries through contraction. This improves the efficiency of exchange between the blood in the capillary and the tissue surrounding it. Blood flow into the capillaries is controlled by precapillary sphincters, smooth muscle bands that wrap around metarterioles.

---

* Corresponding author: Ahmed N Ghanem

Egypt Retired Consultant Urologist Surgeon & Independent Investigator 10 Merton Court, Faculty of Medicine, Mansoura University, The Strand, Brighton Marina, BN2 5XY. The UK.

The purpose of capillaries is to play the central role in the circulation, delivering oxygen in the blood to the tissues, and picking up carbon dioxide to be eliminated. They are also the place where nutrients are delivered to feed all the cells of the body.

1.2. Structure

Capillaries are very thin and are composed of only two layers of cells—an inner layer of endothelial cells and an incomplete outer layer of epithelial cells. Surrounding this layer of cells is the basement membrane, a layer of protein surrounding the capillary. It has been estimated that there are 40 billion capillaries in the average human body. Also, it is postulated that if all the capillaries in the human body were lined up in single file, the line would stretch over 100,000 miles.

1.2.1. Number of Capillaries Varies by Tissue Type

The number of capillaries in a tissue can vary widely. Certainly, the lungs are packed with capillaries surrounding the alveoli to pick up oxygen and drop off carbon dioxide. Outside of the lungs, capillaries are more abundant in tissues that are more metabolically active.

1.2.2. Types of Capillaries

There are three primary types of capillaries in the circulation:

Continuous

These capillaries have no perforations and allow only small molecules to pass through. They are present in muscle, skin, fat, and nerve tissue.

Fenestrated

These capillaries have small pores that allow small molecules through and are in the intestines, kidneys, and endocrine glands.

Sinusoidal or discontinuous

These capillaries have large open pores—large enough to allow a blood cell through. They are present in the bone marrow, lymph nodes, and the spleen, and are, in essence, the "leakiest" of the capillaries.

1.3. Function

The capillaries are responsible for facilitating the transport and exchange of gases, fluids, and nutrients in the body. While the arteries and arterioles act to transport these products to the capillaries, it is at the level of capillaries where the exchange takes place.

The capillaries also function to receive carbon dioxide and waste products that are then delivered to the kidneys and liver (for wastes) and the lungs (for exhalation of carbon dioxide).

1.3.1. Gas Exchange

In the lungs, oxygen diffuses from the alveoli into capillaries to be attached to haemoglobin and be carried throughout the body. Carbon dioxide (from deoxygenated blood) in turn flows from the capillaries back into alveoli to be exhaled into the environment.

1.3.2. Fluid and Nutrient Exchange

Likewise, fluids and nutrients diffuse through selectively permeable capillaries into the tissues of the body, and waste products are picked up in the capillaries to be transported through veins to the kidneys and liver where they are thus processed and eliminated from the body.

1.3.3. Blood Flow through Capillaries

Blood flow through capillaries plays such an important part in maintaining the body. The speed of flow is thought "very slow" to allow for the slow "perfusion balance" between the blood in lumen and the surrounding interstitial fluid (ISF) space.

Capillary beds are regulated through autoregulation, so that if blood pressure would drop, flow through the capillaries will continue to provide oxygen and nutrients to the tissues of the body. With exercise, more capillary beds are recruited in the lungs to prepare for an increased need for oxygen in tissues of the body.

The flow of blood in the capillaries is controlled by precapillary sphincters. A precapillary sphincter is the muscular fibres that control the movement of blood between the arterioles and capillaries. It has an important function in regulating the blood flow speed and pressure in the capillary.

1.3.4. Capillary Microcirculation

Regulation of fluid movement between the capillaries and the surrounding ISF tissues is determined by the balance of two forces: the hydrostatic pressure and osmotic pressure. These are known as Starling's forces proposed as hypothesis in 1886 [2] and 1896 [3] which later became Starling's law with equations.

On the arterial side of the capillary, the hydrostatic pressure (derived from the arterial pressure) is high. Since capillaries are "leaky" this pressure forces fluid and nutrients against the walls of the capillary and out into ISF space and tissues, higher near the inlet.

On the venous side of the capillary, the hydrostatic pressure has dropped significantly. At this point, it is the osmotic pressure of the fluid within the capillary (oncotic pressure) that draws fluids back into the capillary.

2. Current engineering microvascular and capillary ultrastructure anatomy, and correct physiology on pressure and RBCs speed or capillary Blood speed (CBS)

Fletcher S. et al [4] stated: "The body's vascular network is organized in hierarchal, tree-like structures with complex and diverse branching configurations designed to efficiently exchange oxygen, nutrients, and waste within and between tissues throughout the body. Large arteries (>6 mm) carry oxygenated blood to smaller arteries (1–6 mm), and then to the arteriolar network (100–1000 µm), and finally into capillary beds (10–15 µm). Tissue engineers have developed numerous methods to fabricate functional vessels with diameters ranging from 1 to 10 mm. The microvasculature is composed of a dense, high-aspect ratio network of capillaries (10–15 µm) located within <100 µm from one another. Clearly, the design considerations and fabrication techniques to recapitulate the function and architecture of the microvascular networks are unlike those used for engineering large vessels. Here, the goal is to fabricate fine capillaries with high-resolution, with diameters of 5–10 µm, a dimension that is two to three orders of magnitude lower than for large vessels. For ideal oxygen and nutrient delivery, engineered tissues require a dense network of microscale capillaries placed within <100 µm from each other."

2.1. A Brief Historical perspective on landmark articles on Starling's hypothesis

The history of capillary haemodynamics started with Staring's reports in 1886 [2] and 1896 [3]. The two main forces of Starling's hypothesis are: the hydrostatic pressure causing filtration maximum near the inlet as based on Poiseuille's work in strait uniform brass tube. The opposing force of oncotic (osmotic) pressure of plasma proteins (albumin) causes absorption. A balance between these two force is presumed to cause a state of "perfusion" balance between the capillary and ISF space. The two similar minor opposing forces in the ISF space are disregarded in this discusion. Landis reported his article in 1927 [6]. He measured the hydrostatic pressures at the arterial and venous ends of the capillary and reported 32 and 12 mmHg, respectively.

Chambers and Zeweifach (1946) [7] wrote: "The muscular component are narrower than most of the true capillaries in the bed", indicating the presence of precapillary sphincter was known then. Pappenheimer and Soto-Rivera [8] reported their research results in 1948. After that Starling's hypothesis was transformed into a low with equations.

In fairness to Professor Starling, who was a great physiologist, these authors [9,10] correctly wrote: "When Starling proposed his hypothesis in 1896 [3], on the capillary interstitial fluid (ISF) transfer and oedema formation he never wrote equations nor proposed a law." Starling's hypothesis was transferred into a law after Pappenheimer and Soto-Rivera report in 1948 [24] despite having serious experimental error. The ultrastructure anatomy of the capillary of the precapillary sphincter and the inter-cellular cleft pores were discovered in 1967, by Rhodin [11] and Karnovesky [12] respectively.The wide intercellular capillary pores nullify the oncotic pressure in vivo. Multiple criticisms of Starling's hypothesis brought about RSP as an attempt for repair [9,10]. Guyton and Coleman in 1968 reported the pressure of the ISF space in a subcutaneously implanted capsule to be -7 cm water [13] that cannot be explained by Starling's forces.

Despite reporting 21 reasons affirming Starling's law wrong and the correct replacement is the hydrodynamics of the G tube [14-17], Starling's law has remained accepted till curent time of writing this report despite being proved wrong [18,19]. There are hard critics who still believe the Revised Starling's Principle (RSP) is the saviour of Starling's hypothesis [10,11]. Professor Hahn has recently criticized RSP in an article titled: "The Extended (Revised) Starling principle needs clinical validation." I have put my mark on this debate by reporting an article titled: "Revised Starling's Principle (RSP): a misnomer as Starling's law is proved wrong." [6]. I agree with Hahn et al, but I think that their call for further clinical validation of RSP is unnecessary. I predict and warn authors that further clinical validation of RSP or any related research will prove to be total waste of energy, money, efforts, and time. The authors have already regretted using the word "Revised" and introduced "Extended" instead, but their regret will be greater when they realise that both Starling's law and RSP are wrong.

What is unknown about the capillary?

2.2. Missing data from precision engineering microvascular and capillary ultrastructure anatomy, and correct physiology on pressure and RBCs speed or CBS and suggestions for future research

In 1983, Mattfeldt and Mall [5] reported on ultrastructure dimensions of capillaries: "The 'ideal' capillary is a tube connecting an arteriole to a venule. According to Crogh's model it is a perfect, anisotropic, straight, and unbranched tube with a diameter of 7-18 μm." As the capillaries are actually partially anisotropic, curved, branching cylinders with variable cross-sectional area, a geometrical bias arises from the model-reality discrepancies."
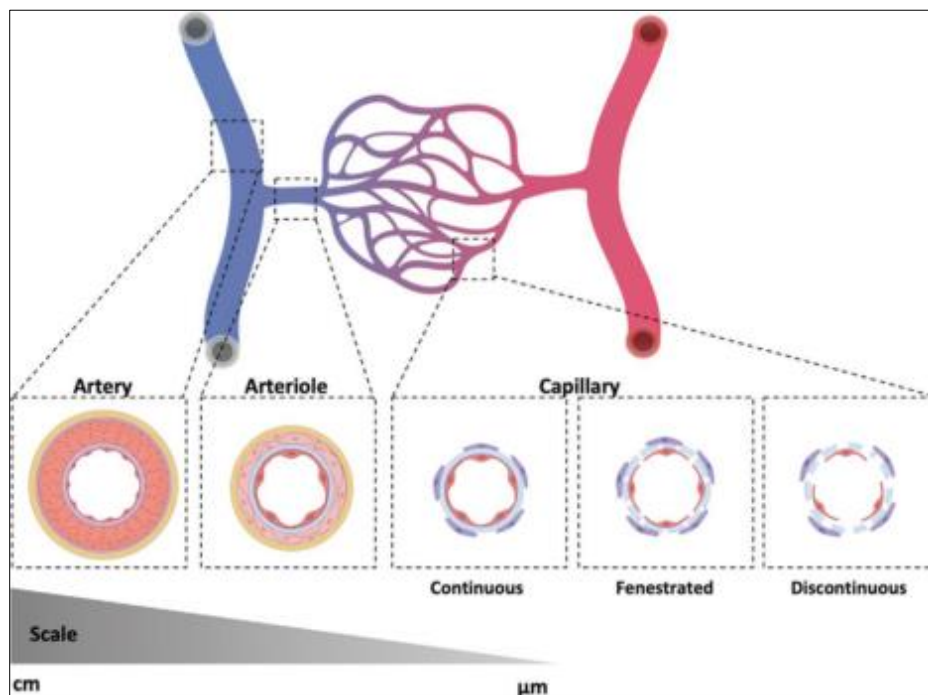
Figure 1 Organization of the vascular tree. The vascular tree is organized into a hierarchical network of arteries, arterioles (blue), capillary beds, veins, and venules (red) that span several orders of magnitude in diameter. All vessels are characterized by an inner layer of endothelium and an outer layer of basement membrane. Arterioles and venules are further bound by a second layer of SMCs as well as elastin and collagen fibres. Capillaries have a varying extent of basement membrane and pericyte coverage and can be continuous, fenestrated, or discontinuous. Figure reproduced from article [20] with its legend stating. Created with BioRender.com

Based on data and diagram reported by Fleisher et al [4] reproduced here as (Figure 1) the diagram is a representation of the structure of the capillaries, but lacks the engineering precise measurements on diameters, length, and number of capillaries and branches with diameters measurements also. Ideally if feasible an actual photograph with the mentioned measurements is better. The terminal arteriole and its capillaries' pressure and RBCs speed also need to be determined in future studies at both the arterial and venous ends. Such data when available allow an actual estimation of the number and cross section areas of all capillaries in relation to the aorta in a human or animal. This summary of the currently missing or unknown data on capillary physiology is so vital for understanding the hydrodynamics of the capillary physiology that it should direct future research. Also, for no obvious reasons the authors swabbed the red colour of

arteriole with the blue colour of venule. The original and natural colour of red should be attributed to the arteriole as it contains red oxygenated blood. The blue colour should be attributed to the venule as it contains blue deoxygenated blood.

Syed MN. et al (2017) [20] reported relevant and important data on the aorta: "The mean diameter of the ascending aorta (Asc Ao) in men was 2.91±0.40 cm, compared with 3.34±0.34 cm in prior studies. The mean diameter of Asc Ao in women was 2.70±0.36 cm, compared with 2.98±0.34 cm in prior studies.". The estimated number of capillaries in adult human has a huge range between 300 million and 40 billion capillaries. Considering the first number as more realistic and a capillary diameter of 10 μm the total cross section area of the capillaries can be calculated and compared to the aorta. My calculation revealed a cross section area of the aorta is 6.6 cm^2 and the sum of total cross section area of all capillaries is 2.375 cm^2. That is considerably less not more than the aorta.

The reported RBCs speed or CBS is generally received as being "very slow". The speed varies from capillary to another and from report to another both in humans [21], and in rats [22-25]. Such variation is expected even in the same capillary from point to another as there is a speed gradient from the precapillary sphincter with a speed of 8.7 mm/s to exit of the capillary with a speed of 4.7 mm/s [22]. What matters most here is the speed gradient along the wide lumen of the capillary tube (wider than the precapillary sphincter of 5 μm in diameter, but not the feeding arteriole).

Ivanov et al (2020) [25] reported: "The mean linear red cell velocity for 100 cerebral capillaries 2–5 μm in diameter was found to be 0.79 ± 0.03 mm/sec. In the temporalis muscle the velocity was equal to 1.14 ± 0.04 mm/sec in 123 capillaries and 2.43 ± 0.08 mm/sec in 34 arterioles and pre-capillaries not more than 5 μm in luminal diameter."

Ishikawa et al (1998) [23] reported: "Average RBC velocity in the capillary is between 0.73 and 0.99 mm/s."

Guevara et al (2016) reported [24]: "The mean centreline RBC velocity in normal rats varied between 1.0 and 9.0 mm/s (most of the measurements were taken in vessels ranging between 20 and 80 μm in diameter). As the diameter of the pial artery becomes smaller, the blood flow rate (pi x (diameter/2)2 x (mean centreline velocity/1.6)) tends to become smaller."

Stücker et al (1996) [21] reported on Resting capillary Blood Velocity in humans: "The mean capillary blood velocity (CBV) rest was 0.47 mm/sec (SD ± 0.37 mm/sec, range 0.14 to 0.93 mm/sec). The average intraindividual difference between max rCBV and min rCBV was 0.30 mm/sec (SD ±0.18 mm/sec). The maximum difference between the capillaries of a single subject ranged up to 0.63 mm/sec."

Stücker et al (1996) also observed [21]: "Another reason for slow CBV may be that the velocity was assessed in the venous limb of the capillary loop, whereas usually CBV is lower than the velocity in the arterial limb, as in our device the venous and arterial capillary limbs of the capillary loop are sometime relatively hard to distinguish." This observation affirms the speed gradient of RBCs speed along the capillary from the sphincter to the exit.

Grubb et al (2020) [22] did not do direct measurements of CBS or RBCs speed and pressure neither at the arterial nor the venous end of the capillary. The values reported by Grubb et al (2020) [8] are derived from formulae above the graph (Fig.2g) (Figure 2) where they stated in the legend: "At rest, the average RBC velocity through precapillary sphincters was 8.7 ± 0.6 mm/s (Fig. 4c), significantly higher than for the bulb (3.6 ± 0.6 mm/s) and the first order capillary (4.7 ± 0.6 mm/s), but correlated with the relative differences in the resting diameters of the vessel segments."

Off course the RBCs speed is correlated with the diameters of the precapillary sphincter and that of the capillary lumen specifically at exit. The remaining wide diameter part of the tube has different RBCs speed according to the gradient between the high figure at precapillary sphincter and the low figure at the exit of the capillary. This is related to the fluid jet's dynamic diameter that changes from 5 μm as rest diameter of the precapillary sphincter at inlet to 10 μm as the diameter of the capillary tube. It is the diameter of the jet in the lumen of the wide section tube that operates in the equation along the whole length of the wide section of the capillary.

Grubb et al [22] derived the above values from the equation show in (Fig. 2g) (Figure G2) that is derived from Poiseuille's law (Figure G3) or perhaps from Bernoulli's equation, where V1A1=V2A2. So, V2=V1 A1/A2 (Figure G4).

Figure 2 The microvasculature tree of head and neck showing arterial branching down to terminal arterioles but not the capillaries. It looks obvious that counting the number of terminal arteriole and the capillaries and calculating its total cross section area is a daunting impossible task. Yet it is possible and easier than one might think. It may be easier only when the TBL applies, please see text
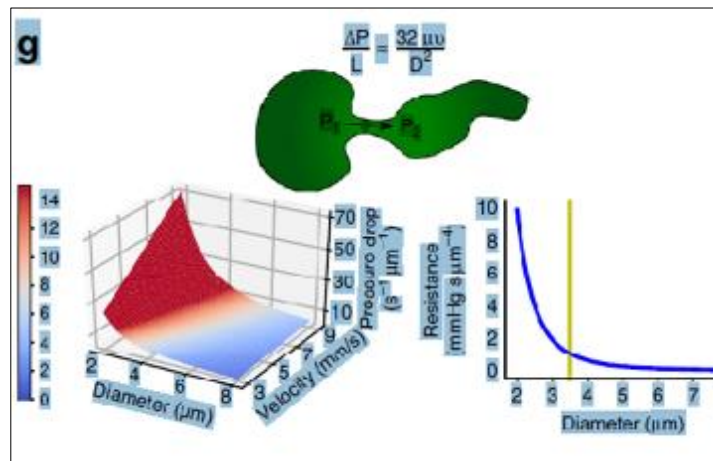

Figure G2 The equation and graph reproduced from Grubb et al article [2] (Fig. 2g).

The authors stated in the figure's legend: "At rest, the average RBC velocity through precapillary sphincters was 8.7 ± 0.6 mm/s (Fig. 4c), significantly higher than for the bulb (3.6 ± 0.6 mm/s) and the first order capillary (4.7 ± 0.6 mm/s), but correlated with the relative differences in the resting diameters of the vessel segments. As shown in Fig. 2g, high RBC velocity through the narrow lumen of the precapillary sphincter amplifies the reduction in pressure across the sphincter due to high shear, i.e., augments the reduction of pressure from larger proximal PAs to downstream capillaries. From the baseline measures, the pressure drop per unit length is 4-times larger in the sphincter than the first order capillary, assuming that RBC velocity and fluid velocity are equal (see Fig. 2g). During whisker stimulation (Fig. 4), both diameter and RBC velocity increased in each segment, but significantly more at the precapillary"

$$\text{Poiseuille's law } \left(\Delta P = \frac{8\mu L Q}{\pi r^4}\right)$$

**Figure 3** Poiseuille's law equation
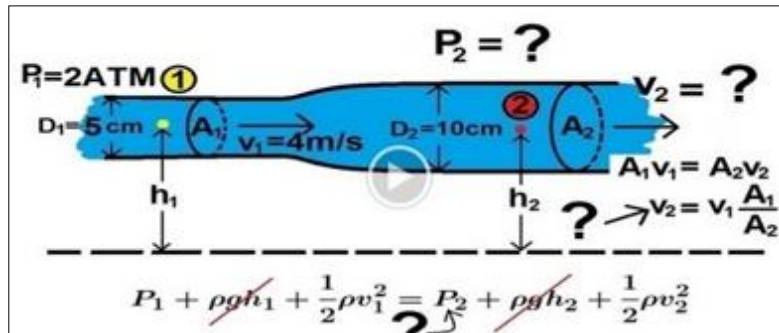
Figure 4 Bernoulli's equation applied to the wide section of the tube after fluid passes through a constriction such as the G tube orifice and the precapillary sphincter.

The figure is reproduced from YouTube by Professor Michel van Biezen [YouTube, Michel van Biezen, lectures, https://youtu.be/VA03j6t5F-8,https://youtu.be/LMDxv96XluY,https://youtu.be/cUMspps8d8A]. [https://www.youtube.com/watch?v=VA03j6t5F-8&t=4s]

Bernoulli's equation persistently gives a single low value of steady speed in the wide section of the capillary tube. The same formula yields low CBS or RBCs speed for the whole wide section of the tube but may only apply at the distal end of the capillary. The equation certainly does not apply at the precapillary sphincter, bulb, or the proximal capillary where we know the speed at the precapillary sphincter is high of 8.7 mm/s and at the capillary exit is 4.7 mm/s. So, there is a definite descending speed gradient along the capillary (Figures G5). The SP is also negative causing suction at the orifice or precapillary sphincter well known as Venturi's effect. So, a modification of the equation to yield both speed gradient and negative SP gradient is in order, and the graph should show this negative side pressure gradient over the capillary length.
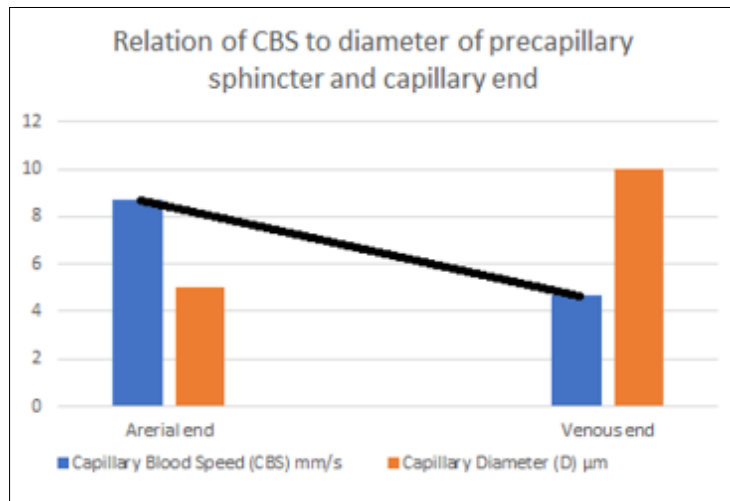
Figure 5 The line representing the CBS or RBCs speed gradient from precapillary sphincter to exit of the capillary. The graph is the same as (Figure 26) was created using Microsoft Excel and the black line added in Paint. Any point along the black line can predict the RBCs speed or CBS at a given length along the capillary, by dropping a vertical line on the vertical Y axis

So the dynamic variables in an apparently impossible future equation or equations should include:-

- The FP gradient for (FP and ΔFP) for which the measured hydrostatic pressure (MHP) my be used such as that measured by Landis at capillary inlet and exit (MHP$_{inlet}$ and MHP$_{exit}$).
- The SP gradient for (SP and ΔSP) as measured in the G tube (Figure 17,18)
- The fluid jet diameter (D$_j$) at precapillary sphincter and at exit (D$_{j\,inlet}$ and D$_{J\,Exit}$) (Figure 5).
- The fluid jet length (L$_j$) (Figure 17) and tube length (L).

- The CBS or RBCs speed at start and end of the capillary (CBS$_{inlet}$ and CBS$_{exit}$) as suggested to be done in future at both arterial and venous ends of the capillary by Stucker et al [21].

However, as all the above dynamic variables are measurable the equation may be easier than one might think. [14].

- The low PP shown in (Figure 6) demonstrating the hydrodynamic of the porous orifice (G) tube is 24 cmH2o that is lower than the measured hydrostatic pressure (MHP) measured by Landis [6] at the arterial end of the capillary of 32 mmHg and is certainly adequate for inducing the dynamic FP and SP in the capillary as shown in the G tube later (Figure 7).
- In the capillary as in the G tube, the speed of flow in the capillary shown in Dr Mayrovits' video is "very fast" < http://fluidphysiology.org/2020/05/25/more-on-ghanems-hypothesis/> < https://youtu.be/QuWhKN1bHLA >., and certainly cannot be described as "very slow" as generally believed and taught in current classical teaching on the capillary circulation, so there is no "diffusion" here and the word must be corrected in the title of this article [22].
- The fluid transfer of the G-C model (Figure 7) occurs according to a precise fast circulation of fluid between the G tube lumen and s urrounding chamber C. This must also occur in the capillary, not the slow diffusion that provide good adequate irrigation of the ISF space without oedema formation. This fast capillary-ISF circulation can account for the cell demand at rest and for higher demand of oxygen and nutrient delivery with removal of waste products during strenuous physical activity.
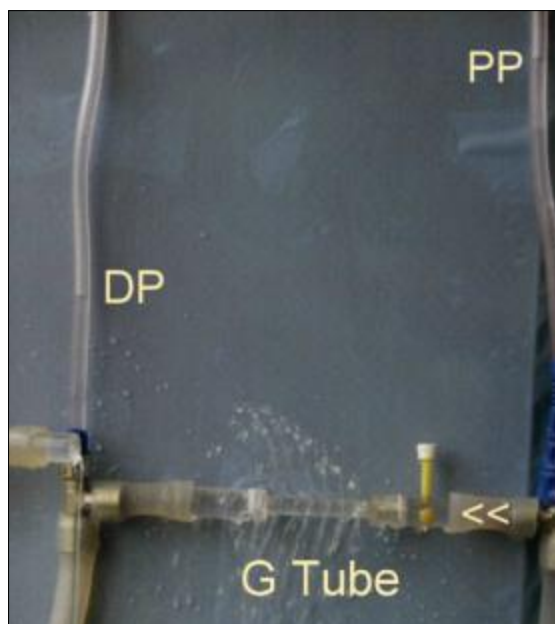
Figure 6 The hydrodynamic of the G tube (without surrounding chamber)

Connected to a garden hose. It shows lower PP of 24 cm water and DP of 12 cm water and the side pressure gradient higher positive maximum at exit. The negative SP near the inlet is not shown here but is demonstrated elsewhere (Figure 7, 10). The pressure gradient also demonstrates the direction of flow in the G tube from right to left hand side. The system is continuously overfilled from a water hose to replace the water loss from the holes of the G tube. Please, note that the proximal and distal pressures before and after the G tube shows values of 24 and 12 cm water, respectively, that are lower than and equal to measured pressure at proximal and distal ends of the capillary obtained in a real capillary by Landis of 32 and 12 mmHg (see text) and still induce the G tube phenomenon.
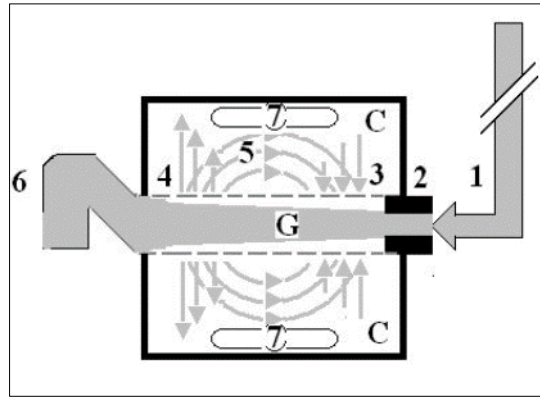
Figure 7 A diagrammatic representation of the hydrodynamic of G tube based on G tubes and chamber C seen in Figure 5. This 38-years old diagrammatic representation of the hydrodynamic of G tube in chamber C is based on several photographs. The G tube is the plastic tube with narrow inlet and pores in its wall built on a scale to capillary ultra-structure of precapillary sphincter and wide inter cellular slit pores, and the chamber C around it is another bigger plastic tube to form the G-C apparatus. The chamber C represents the ISF space. The diagram represents a capillary-ISF unit that should replace Starling's law in every future physiology, medical and surgical textbooks, and added to chapters on hydrodynamics in physics textbooks.

The numbers should read as follows:

- The inflow pressure pushes fluid through the orifice
- Creating fluid jet in the lumen of the G tube**.
- The fluid jet creates negative side pressure gradient causing suction maximal over the
- Proximal part of the G tube near the inlet that sucks fluid into lumen.
- The side pressure gradient turns positive pushing fluid out of lumen over the distal
- Part maximally near the outlet.
- Thus, the fluid around G tube inside C moves in magnetic field-like circulation (5)
- Taking an opposite direction to lumen flow of G tube.
- The inflow pressure 1 and orifice 2 induce the negative side pressure creating the dynamic G-C circulation phenomenon that is rapid, autonomous, and efficient in moving fluid and particles out from the G tube lumen at 4, irrigating C at 5, then sucking it back again at 3,
- Maintaining net negative energy pressure inside chamber C.

**Note the shape of the fluid jet inside the G tube (Cone shaped), having a diameter of the inlet on right hand side and the diameter of the exit at left hand side (G tube diameter). I lost the photo on which the fluid jet was drawn, using tea leaves of fine and coarse sizes that runs in the center of G tube leaving the outer zone near the wall of G tube clear. This may explain the finding in real capillary of the protein-free (and erythrocyte-free) sub-endothelial zone in the Glycocalyx paradigm. It was also noted that fine tea leaves exit the distal pores in small amount maintaining a higher concentration in the circulatory system- akin to plasma proteins.

What is wrong with capillary physiology?

Mentioned above in the received knowledge on capillary physiology there is one wrong physiological law and 2 misconception which are:

- It is generally accepted that Starling's law regulates the capillary-ISF transfer.
- It is postulated that the cross-sectional area of capillaries is larger than that of the Aorta. Some sources even say that the cross-section area of all capillaries of one average muscle is greater than the aorta!
- It is also assumed that the RBCs speed or CBS is "very slow" to allow for the slow perfusion to take place according to Starling's forces.

The next part shall provide substantial evidence to prove Starling's law is wrong and the correct replacement is the hydrodynamic phenomenon of the G tube of magnetic field-like fluid circulation occurring between the capillary blood in lumen and the surrounding ISF space. Also, the new Tree Branching Law provide the evidence to prove that the "cross section of all capillaries is greater than the aorta", and the RBCs speed is "very slow" are both wrong misconceptions.

What is new about capillary physiology?

- The hydrodynamics of the porous orifice (G) tube as the correct replacement [14-17] for the wrong Starling's law for the capillary-ISF transfer [18,19] and its clinical importance in recognizing two new types of volumetric overload shocks (VOS) [29,30] and its role in the patho-aetiology of the acute respiratory distress syndrome (ARDS) [31-33] are summarized here.
- The Tree Branching Law (TBL) and its role in correcting two misconceptions on the red blood cells (RBCs) speed in capillaries being too slow and the total cross section areas of all capillaries being larger than the aorta' cross section area are reported here.

2.3. The hydrodynamics of the G tube:

The hydrodynamics of the G tube was reported as prelimenary report at Medical Hypothesis in 2001 [14] demonstrating its relevance to the haemodynamics of the capillay and as well as its clinical significance proposing the G tube phenomonon of magnetic fieeld-like fluid circulation between the capillary lumen and ISF space as the correct replacement for Starling's law and hypothesis [14-19]. My contributions on the subject of G tube physics and capillary physiology [14-19], identifying two new vascular shocks [29,30] and resolving the puzzle of ARDS [31-33] are reported. Not only the exact patho-aetiology of ARDS was identified but also a possible preventable and curable therapy was suggested [31].

3. Hydrodynamics of the G tube: What are the new physics discoveries of physiological relevance?

The new hydrodynamics of the G tube with relevance to capillary physiology are summarised here.

The results of the G tube study clearly indicate and recognize the following new discoveries:

- There is a major difference between the hydrodynamic of Poiseuille's tube and that of the G tube demonstrated by comparing the two tubes working in isolation (Figures G8 and G9) and connected to a circulatory model (Figure 10 and 11), showing Poiseuille's tube and G tube hydrodynamics, respectively.
- There is also a difference between the hydrostatic pressure of a stagnant fluid and the hydrodynamic pressures of FP and SP of a moving fluid.
- The lumen pressure components of the dynamic fluid flow of FP and SP are precisely identified and measured in both Poiseuille's tube and the G tube both in isolation and when connected to a circulatory model.
- The SP in the G tube causes negative pressure gradient exerted on the wall maximum near the inlet (Figure G12) and turns positive pressure maximum near the exit (Figure G9, G11).
- Thus, in the G tube suction or absorption of fluid occur through side holes near the inlet while filtration occurs through holes near the exit.
- This creates the unique autonomous rapid dynamic magnetic field like fluid circulation in a surrounding chamber (C) between fluid around the G tube and fluid inside its lumen (Figure G7).
- The negative SP of the G tube creates net negative pressure in chamber (C).
- The flow in chamber C is in the opposite direction to the flow of fluid in the G tube lumen as shown in.
- The G tube's magnetic field like fluid circulation phenomenon between fluid inside its lumen and that surrounding it in chamber C works in both macro and micro tubules, such as the capillary, alike as based on the physiological evidence [10] and other evidence presented here.
- The presumed slow RBCs speed as it passes through the capillary is incorrect. Modern videos on the speed of flow in the capillary circulation shows RBCs running fast (The video is reported by HN Mayrovits < http://fluidphysiology.org/2020/05/25/more-on-ghanems-hypothesis/> < https://youtu.be/QuWhKN1bHLA >. The speed of RBCs or capillary blood speed (CBS) in the capillary shown in this video is fast enough to induce the magnetic flow phenomenon of the G tube in the capillary and its

surrounding ISF space. The speed of flow in the capillary shown in this video is "very fast", and certainly cannot be described as "very slow" as generally believed and taught in current classical teaching on the capillary circulation. As mentioned here later the RBCs speed or CBS is 8.7 mm/s at the pre-capillary sphincter and 4.7 mm/s at the exit of the capillary reported Grabbs et al in rats [22] and in humans with uncanny similarity after correction [21]. The speed gradient between the two recorded speeds is that that matters in inducing the G tube magnetic field like phenomenon in the capillary.

- The RBCs speed or CBS run down a slope of gradient from pre-capillary sphincter to exit of the capillary, from 8.7 mm/s to 4.7 mm/s [2] (Figure G5). This speed gradient induces the magnetic fluid-like flow phenomenon of the G tube between the blood flow in capillary lumen and the surrounding ISF space. This FAST capillary-ISF transfer is essential for the viability of tissues and cells under rest conditions and strenuous exercise. Substantial evidence on this issue with supporting graphs is reported here, particularly as the driving pressure in the capillary of 32 mmHg [2] is higher than proximal pressure in the G tube of 24 cm water (Figure 6).

Thus, the hydrodynamics of the G tube demonstrate that the dynamic pressure of a moving fluid has 2 pressure components that are different from the hydrostatic pressure of a stagnant fluid:

- The flow pressure (FP) that is in the direction of flowing fluid measured with a cannula or needle facing up stream. It exists in both Poiseuille's and the G tube and is high positive pressure gradient (Figure G13).
- The side pressure (SP) that is lower than FP in Poiseuille's tube and is measured with a cannula or needle facing downstream or sideways.
- The negative SP is unique to the G tube causing negative pressure gradient and suction over the proximal part of the G tube maximum near the inlet (Figure 7,12,14) and turns gradually into positive pressure gradient maximum near the exit (Figure 9,11).

Both FP and SP of a dynamic flow are different from the hydrostatic pressure measured with a cannula occluding the lumen of the tube. This is named here as the MEASURED hydrostatic pressure (MHP) of the tube flow as measured by Landis in the capillary [6], which induce the SP gradient that induces the magnetic field-like phenomenon of the G tube in the capillary as shown in (Figure G7). The G-C apparatus connected to a circulatory model and demonstrating the hydrodynamics of the G tube is shown in (Figure G15).
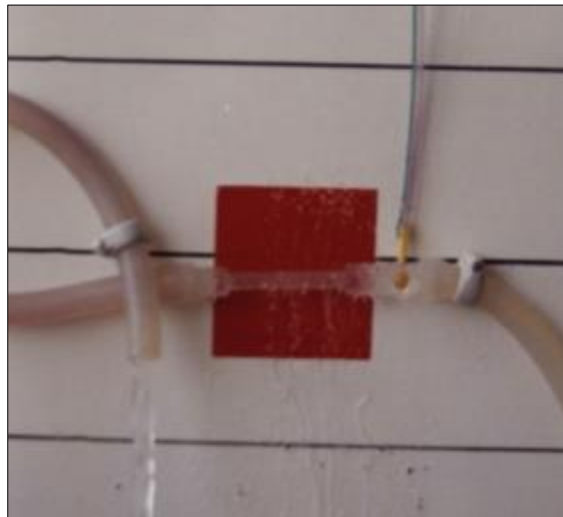
Figure 8 Poiseuille's tube hydrodynamic with positive side pressure along the entire length of the tube causing fluid to filter out maximum near the inlet and minimum near the exit. This is what Starling had based his hypothesis on regarding the hydrostatic pressure causing filtration maximum near the orifice. This will be compared to the hydrodynamic of the G tube (Figure 9) built on a scale to capillary ultrastructure of pre-capillary sphincter and intercellular slits making wide capillary pores that allow the passage of molecules larger than plasma proteins
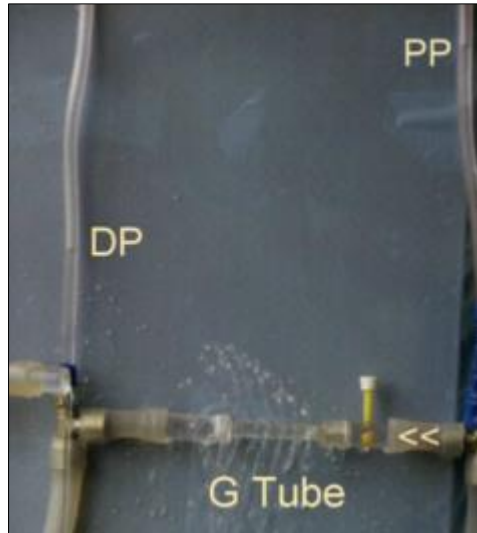
Figure 9 The hydrodynamic of the G tube's with side pressure gradient lower at the inlet where it is negative and turns into positive pressure maximum near the exit, with visible magnetic field-like circulation around it seen at your top right hand quarter of the photo-based on which and other photos shown below, the diagram showing the G-C circulation was drown (Figure 4). There is negative side pressure gradient over the proximal part of G tube not shown here but is shown in Figure 10


Figure 10 The same circulatory system shown above but without orifice of the tube i.e. this is a (Poiseuille's tube). The DP (venous pressure or (CVP) increases to 19 cm H2O, the PP (arterial) drops to about 35 cm H2O, and the CP (akin to ISF pressure) increases to levels above DP of 22 near orifice and 21 near exit. This increases volume and pressure in chamber C-akin to oedema formation. The flow in chamber C is the same direction as in Poiseuille's tube. This is akin to volume kinetics of VOS in ARDS

Connected to a garden hose. It shows lower PP of 24 cm water and higher DP of 12 cm water and the side pressure gradient higher positive at exit. The negative side pressure near the inlet is not shown here but is demonstrated elsewhere. It also demonstrates the direction of flow in the G tube from right to left of your hand side. The system is continuously overfilled from a water hose to replace the water loss from the holes of the G tube. Please, note that the proximal and distal pressures before and after the G tube of 24 and 12 H2O, respectively, are lower than and equal to mean pressure at proximal and distal pressure figures obtained in a real capillary by Landis of 32 and 12 mmHg (see text) and still induce the G tube phenomenon as shown in (Figures 1).

Figure 11 The hydrodynamic of the G tube (without surrounding chamber)
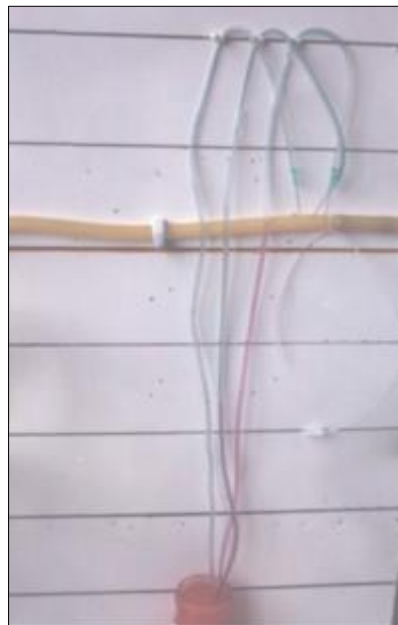
Figure 12 A rubber orifice tube's negative side pressure gradient maximum near the inlet, turning into positive pressure maximum near the exit as shown in figure 2, with visible magnetic field-like circulation around it seen at your top right hand quarter of the photo- based on which and other photos shown here, the diagram showing the G-C circulation was drown (Figure 1). This rubber orifice tube was also used for measuring the flow pressure (FP) and side pressure (SP) which are dynamic components of the lumen pressure (LP) induced by the proximal pressure (PP)- akin to arterial pressure
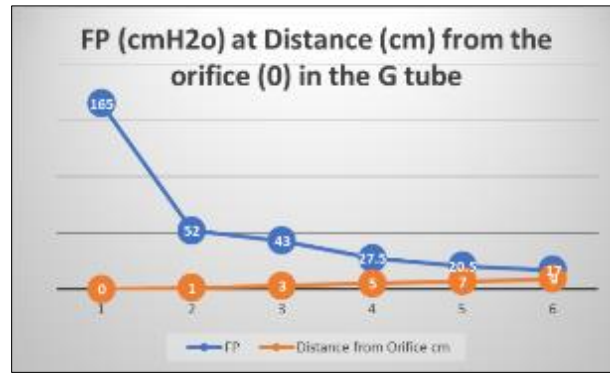
Figure 13 The flow pressure (FP) in cmH$_2$0 in the G tube at distance in cm from the orifice at point 2. The high pressure at point 1 is FP of Poiseuille's tube. It demonstrates FP descending gradient from orifice at point 2 to that along the G tube length from points 2-6
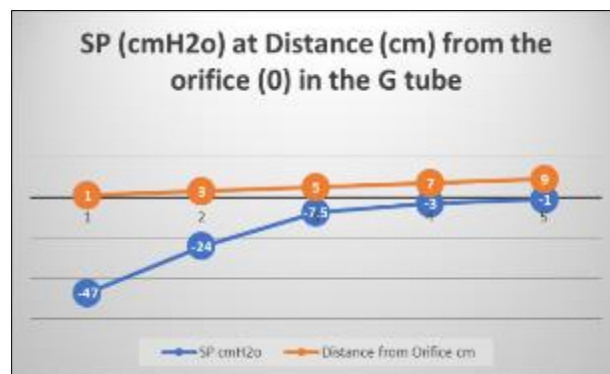
Figure 14 The side pressure (SP) in cmH$_2$o at cm distance from the orifice at 0 (not shown). Measurements started at 1 cm then at increasing distances of 3, 5, 7 and up to 9 cm. It shows a negative pressure gradient along the G tube over the proximal half that turns into positive pressure gradient maximum at the distal end (exit) as shown in (Figure 3)

Figure 15 The G tube in G-C apparatus connected to circulatory model driven by electric pump. The proximal pressure (PP) akin to arterial pressure is above 100 cm water when the distal pressure (DP) is less than 7 cm water (hidden behind the blue tube). The pressure in the chamber around the G tube is less than DP. Furthermore, the pressure in C manometers is lower near the inlet than it is near the exit. So, suction or reabsorption of fluid occurs through side holes

near the inlet while filtration occurs through side holes near the exit. This creates the dynamic magnetic field like circulating fluid inside G tube (capillary) with that in the surrounding C that has net negative pressure akin to ISF space that gets well irrigated without oedema formation. Irregularities of the inner surface of the G tube perturbed the G-C circulation and caused elevation of pressure in C akin to oedema formation, this may explain the importance of Glycocalyx; being normally smooth but sepsis causes irregularities. Also elevating DP akin to elevated CVP augments oedema formation as does low PP akin to hypotension of the circulatory system.

4. The physics and physiological relevance of the hydrodynamic of the G tube to the haemodynamic of the capillary spicifically Starling's law on the capillary-ISF transfer

This has been previously reported [14-17] and affirmed here. The clinical significance of applicability of the hydrodynamics of the G tube to the patho-aetiology of the new volumetric overload shosks (VOS) [29] were also reported as volume kinetic shocks [30] causing ARDS [31-33].

4.1. The Tree Branching Law (TBL)

The TBL is defined as and states that: "The trunk of a branching tree does not, and cannot, give rise to branches that have sum of all its cross-section areas larger than its own". In other words: "The sum of all tree branches' cross-section areas at any level is less than its own trunk."

This TBL was originally based on observational theory on green trees and red vascular trees of the aorta and its arterial branches but has now been investigated and validated. The results of scientific, mathematical, and experimental evidence show that TBL is validly correct on all green and red trees as summarized here. This law rule applies further down the arterial tree to the terminal arterioles and capillaries, and up a green tree to its leaves as a branch becomes a mother trunk for its own sibling branches.

The TBL is not just a scientific curousity of trivial importance but very important for understanding capillary physiology. It verifies that the cross-section areas of the sum of all functional capillaries is less than that that of the aorta. This is the scientific basis that corrects the misconception that the cross section areas of the capillaries is "much greater" than the aorta- based on which the predicted RBCs speed is thought "very slow", while in reality it is proved fast. The speed gradient of RBCs speed along the capillary must account for the magnetic field-like fluid circulation around the capillary as it occurs in the G tube (Figure 7) [17]. Furthermore, the TBL will allow accurate calculation of the capillaries in a human or animal based on data concerning the aorta' maximum diameter and its cross section area and capillaries' diameters. Currently this seems a daunting idea as based on this photograph of the microvascular tree of the head and neck (Figure 2). However, this shall prove feasible in the light of the new TBL reported here, when the precision engineering data on terminal arteriole's measured diameter and its number of capillaries with its measured diameters become available in a true to life arteriole-capillaries-venule diagram or picture. The currently reported diagram on the arteriole-capillaries-venule unit (Figure G1) [20] lacks the above mentioned engineering precision data measurements, and wrongly swabs the colours of red and blue for the arteriole and venule.

The TBL was investigated and validated by the study investigations of all types of known trees which all proved TBL is valid and correct; it included the following trees.

- The Fiber-Optic Light Tree (Figure T1)

The cross section area of all fibres gathered in a trunk is 86.625 mm^2. The cross section areas of all fibres individually calculated and summed up later is 62.857 mm^2. So, the sum of cross section areas of all fibres individually is less than (72.562%) the trunk of all fibres gathered in one bundle- a rather surprising result as I initially though it might be equal.

- The Green Trees

Figure 16 The Fibre-optic tree and Digital Vernier Calibre for precise measurements. This tree obeys the TBL. The sum of all fibres as individuals are less than the all fibres gathered in one trunk: a surprising result- see text!?

4.1.1. Household Miniature Croton Tree (Figure 17)

Figure 17 Miniature Household Croton Tree. It applies the TBL down to and including the terminal branches. The leaf stems, however, represent an exception to the law perhaps because it represents terminal function unit rather that the transport conduit that all branches represent.

The cross section area of the trunk is 106.27 mm². The cross section areas of all the 1st order branches is 96.28 mm². (90.599%) The cross section areas of all 2nd order terminal branches is 94 mm². (88.454% of the trunk) As branching continue, the cross section of all branches is less than its own mother branch, as well as being much less than the tree trunk. These findings were confirmed in all trees examined.

4.1.2. Nature Big Green Trees

Samples representing all big trees of Gardens, Streets and Forest were studied. All types of trees obey TBL as in all trees the sum of cross section areas of all branches is less than that of the trunk (Table 1) and a descending trend extends to the terminal branches where leaves originate.

Table 1 Data for the 6 big trees on diameters and cross section areas. The trunk cross section area is compared to the sum of all branches are shown in red for comparison. All the big green trees obey TBL and have total cross section area of all branches that less than that of the trunk

	Trunk D	**Trunk Area**	**All Br Area**	**Br 1**	**Br 2`**	**Br 3**	**Br 4**	**Br 5**	**Br 6**	**Br 7**
Tree 1	10.65	89.118	70.295	4.08	4.04	4.66	4.06	3.45	4.89	
Tree 2	5.4	22.911	16.467	0.63	2.05	3.3	3.02	1.5	0.54	1.62
Tree 3	5.5	23.768	23.085	3.03	3.13	3.69	2.91			
Tree 4	7.71	46.706	40.352	2.2	1.69	1.52	5.4	2.52	0.76	1.11
Tree 5	6.89	37.300	26.755	2.54	3.89	5.95	3.21			
Tree 6	7.79	47.680	21.254	2.4	1.34	1.7	1.1	1.28	4.08	2.37

The street tree (Tree1) gives a good representation of the TBL as it has bare branches up to the 3rd level branches. The trunk of (Tree 1) based on (Figure T3) has a cross section area of 101.218 mm^2 and gives rise to 2 branches of 1st order that have a sum of cross section areas of 83.958 mm^2. (82.948%) The total cross section area of the 2nd order branches that were 6 branches, 3 from each mother 1st order branch, have total sum of cross section areas of 64.661 mm^2. (63.883% of the trunk) The same trend continues up the green tree to the level of terminal branches where the leaves originate.


Figure 18 A street tree (Tree 1) with bare and measurable branches' diameters up to the 3rd order. It all applies the TBL

5. The Red Aorta's Tree

5.1. Aorta's Arterial tree in Humans (Figure T4)

The aorta gives rise to 1st order branches of 45 arteries that have different diameters (Table 2). The ascending aorta's maximum cross section area is 112.202 mm^2 -based on measurements taken from (Figure T4). The measurements of diameters were taken on the outside diameter of aorta and arteries. The 1st order arteries (directly branching from the aorta) have a total sum of cross section areas of 105.86 mm^2. (94.348%) So, the arteries have cross section areas that is less than the aorta. The same rule applies to all further down branching of arteries down to and including the terminal arterioles and precapillary sphincters.
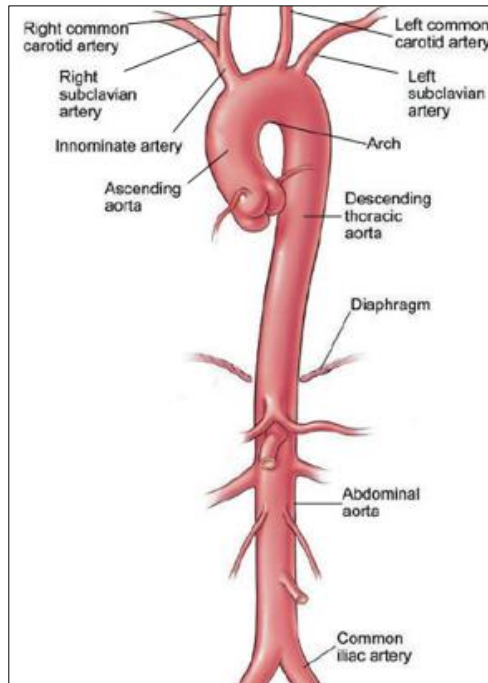
Figure 19 The Aorta (Trunk) and its main first level arteries (Branches). The aorta gives rise to 45 first degree order arteries that vary in diameters but are all measurable, hence the cross-section area is calculated and compared to that of the aorta which is less than the aorta trunk. It applies the TBL. When the precise engineering measurement data on terminal arterioles and capillaries become available it should be possible to calculate an approximate correct number of capillaries based on known capillary diameter and its number arising from the terminal arteriole. (This f1gure is reproduced from an article on the aorta by Cleveland clinic.)

Table 2 The data on the aorta and its branching arteries. The number in bald red compares the cross-section area of the aorta to the total number of branches' cross section areas

Showing or Not	Aorta D	Branch Name	Br No	D	A mm^2	Total Area
Showing	11.95	Coronary	2	1	0.78571429	1.57142857
Showing	5.975	Innominate A	1	3.96	12.3212571	12.3212571
Showing		L Common Carotid A	1	2.56	5.14925714	5.14925714
Showing		L Subclavian A	1	2.57	5.18956429	5.18956429
Showing		Coeliac A	1	4.18	13.7283143	13.7283143
Showing		Super Mesenteric A	1	2.4	4.52571429	4.52571429
Not Showing		Suprarenal A	2	0.5	0.19642857	0.39285714
Showing		Renal A	2	2.9	6.60785714	13.2157143
Showing		Gonadal A	2	1	0.78571429	1.57142857
Showing		Infer Mesenteric A	1	2	3.14285714	3.14285714
Showing		R Common iliac A	1	5	19.6428571	19.6428571
Showing		L Common Iliac A	1	4.94	19.1742571	19.1742571
Not Showing		Intercostal Arteries	18	0.5	0.19642857	3.53571429
Not Showing		*Infer Diaphragm A*	2	0.5	0.19642857	0.39285714
Not Showing		Lumbar Arteries	8	0.5	0.19642857	1.57142857
Showing		Sacral Artery	1	1.2	1.13142857	1.13142857
	112.202	Total	45			105.864

The measurements of the aorta and its branching arteries were done on a photograph (Figure T4) measuring the diameters of aorta and arteries on the outside. This is to be replaced in a future study by the actual measurements of the inner diameters of the aorta and arteries taken from a hard cast after filling the aortic tree with liquid cement, leaving it to dry and harden up, then removing the walls of the aorta and arteries that can be done on a human cadaver and/or animal models. Such study should validate the TBL results reported here.

5.2. Arteriole-Capillaries-Venule Diagram (Figure 1)

The TBL applies to the aorta and its first order arterial branches and its syubsequent branches of all arteries down to and including the terminal arterioles and precapillary sphincters. The arteries are conduits involved in transporting the blood to capillaries that are the terminal functional units that serve the cells and tissues. Capillaries being the terminal functional units may or may not obey the TBL; the currently known data on arterioles and capillaries [4] are insufficient to finalize this issue for sure now.

A terminal unit of arteriole-capillaries-venule based on preferably an actual photograph if feasible or an engineering precision diagram on ultrastructural anatomy of the arteriole-capillaries unit which show the number of capillaries orginating from the terminal arteriole, giving the capillaries' length and measured diameters, indicating whether it branches or not and the measured diameter of branches if any exist. The pressure and speed of blood flowing inside capillary lumen should be measured at both arterial and venous ends of the capillary. With these data available with known aorta's diameter, it is possible to calculate the most likely numbers of capilleries or at least the functional capillaries in a human and/or animal. Also, the total cross-section areas of all the capillaries can be accurately calculated to define its relation with the aorta's cross-section area. I think that at least the functional capillaries have a total cross section area that is smaller not larger than the aorta. The adequae available evidence for this notion is reported here.

6. The deductive evidence demonstrating that the total cross section area of the capillaries is less than that of the aorta, not more.

Deductive evidence demonstrate that the sum of all terminal arterioles' cross section area is less than the aorta. This is based on the evidence from the TBL that the 1st order branching arteries have a total cross section area that is less than that of the aorta. Furthermore, the 2nd order arterial branches have a total cross section area that is less than the preceeding 1st order arteries and much less than the aorta. The trend continues down to the terminal arterioles. This trend is also seen in green trees. It was observed in every branching tree that the 1st order branches have a cross-section area that is less than that of the trunk. Further branching into 2nd order branches also show that the cross section area is smallar than the preceeding 1st order branches' cross section area and much smaller than the trunk. From this rule it is deduced that the cross section area of all terminal arterioles is less than that of the aorta. The capillaries may follow suit despite its wider diameter that is the double of the precapillary sphincter, but not more than half the diameter of the feeding arteriole diameter. Hence, the cross section area of all capillaries is much less than the aorta.

7. The mathematical evidence demonstrating that the total cross section area of the capillaries is less than that of the aorta, not more.

The precision engineering diagram of terminal arteriole and capillaries (Figure 1) demonstrates that 3 capillaries branch from the terminal arteriole each have a diameter less than half of the arteriole. The diameters of the arteriole is 2.61 mm and of the 3 capillaries it originate from it are 0.48, 1.5 and 1.3 mm which have a cross section area for the arteriole of 5.352 mm^2 and for the 3 capillaries the sum total of cross section area is 3.276 mm^2. (61.211%) This means that the total sum of cross section areas of the capillaries is less than that of the arterioles and therefore much less than that of the aorta, not more.

In the non-existing event of case scenario that an arteriole gives rise to 4 capillaries each has a diameter that is half that of its own then the cross section area of capillaries equals that of the arterioles, not more, and the total cross section areas of all capillaries remain much less than that of the aorta. Almost certainly the cross section area of all the functional capillaries are less than that of the aorta, never more. I am happy with the above provided evidence but do not mind considering it a theory for now to be validated when future precision data on the arteriole-capillaries-venule unit's exact ultrastructure anatomy with measurements becomes available.

8. The clinical significance of replacing Starling's law with the G tube magnetic field-like fluid phenomenon and correcting other misconceptions.

Physiologists and physicists may be reluctant to support the truth brought about by the discovery of the hydrodynamics of the G tube denying its applicability to the capillary hemodynamic, being most concerned about formulae and calculations. Physicians, however, particularly Anesthetists, Surgeon, and Intensivists are most concerned about the lives and safety of their shocked, acutely ill patients and patients undergoing major surgery.

Physicians who must rely on Starling's law for giving intravenous fluid therapy in clinical practice do realize the seriousness of this affair. These Physicians know that Starling's law does not hold in these clinical settings: Being wrong has induced errors and misconceptions on fluid therapy [28]. These errors mislead physicians into giving too much fluid during the resuscitation of shock, acutely ill patients, and prolonged major surgery [29]. It thus induces the volumetric overload shocks (VOS) [31] also reported as volume kinetic (VK) shocks [32] that cause the acute respiratory distress syndrome (ARDS) [33-35] or the multiple organ dysfunction syndromes (MODS).

Not only the exact patho-aetiology of ARDS was identified but also a possible prevention and curable therapy is advanced and recommended [31,32]. So, ARDS is not caused by sepsis and Covid-19 only but also by VOS though remaining unrecognized and underestimated. Sepsis is managable by the use of appropriate and adequate powerful abntibiotics that exist today. Covid-19 that kills its victims by inducing ARDS is transient and will soon go away or a vaccination will materialize that puts it dormant in history like other eradicated infectios diseases by the effective vaccination. Meanwhile, ARDS induced by VOS shall remain unrecognized and underestmated killing hundreds of thousands of patients all over the World each year unless Starling's law is disposed off and better policy on fluid therapy is implemented and every practicing physician in the World particularly those involved in fluid therapy knows about it.

The faulty Starling's law is the primary culprit responsible for the death of hundreds of thousands of ARDS patients every year all over the World [31-33]. This is preventable and curable when the truth on the G tube discovery can prevail and shine. All should welcome the new discoveries in physics, physiology, and medicine [34]. The physics, physiological and clinical evidence is so overwhelming that it justifies saying farewell: "Goodbye Starling's law, hello G tube" [35].

9. Conclusion

This article presents concisely what is known about the capillary ultrastructure anatomy and physiology as is currently tought in medical schools and reported in all physiology textbooks. Yet the this knowledge on capillary physiology has missing data, errenous law and two misconceptions, identified in the what is unkown or missing section and on what is wrong with current understanding of capillary physiology. The section of what is new presents a summary of the G tube discovery of hydrodynamics, how it proves Starling's law is wrong and provides the corrcet replacement of the magnetitic field-like fluid circulation phenonenon for explaining the capillary-ISF transfer. Also the the Tree Branching Law (TBL) corrects the misconceptions that the total cross section areas of all the capillaries is very much greater than the Aorta, and the capillary blood speed is very slow to allow for the slow perfusion equilebrium state between the capillary blood and ISF space as based on the currently received but incorrect Starling's forces.

The currently missing data on capillary physiology include: A representative model of the arteriole-capillaries-venule unit with precise measurements of the arteriole and capillaries diameters and capillary number branches for the accurate calculations for the cross section areas of the capillaries in relation to that of the Aorta. Also the speed of RBCs or CBS shoulkd be measured at both the arterial and venous ends of the capillary.

The section of what is new on the capillary physiology summarises the new discovery of the G tube hydrodynamics provideng the correct replacement for the wrong Starling's law, namely the magnetic field-like fluid circulation that explains well the capillary-ISF transfer that effecientlty provide for the cell and tissue viability at rest and during streneous exercise. The TBL provides substantial evidence that rectifies the misconceptions on capillary cross section areas to show that it is less than that of the Aorta, and speed of blood is really fast to allow for the magnetic field-like fluid circulation between capillary blood and the surrounding ISF space to operate.

The missing data on capillary physiology should direct future research. Correcting the wrong Starling's law and the misconceptions should pave the way for the new magnetic field-like fluid dynamics of of the G tube to improve understanding of and be implemented in the capillary-ISF transfer. These will undoubtedly help in resolving the clinical problems of recognizing the new volume kinetic shocks or volumetric overload shocks causing the acute resiratory

distress syndrome that complicate fluid therapy in hospital practice due the wrong rules being diucated by the wrong Starling's law.

Compliance with ethical standards

References

[1] Eldridge K, Kampalath R. Capillary Structure and Function in the Body.

[2] Starling EH. Factors involved in the causation of dropsy. *Lancet* 1886; ii: 1266–1270, 1330–1334 and 1406–1410.

[3] Starling EH. On the absorption of fluids from connective tissue spaces. J Physiol. 1896; 19: 312-326.

[4] *Sharon Fleischer, Daniel Naveed Tavakol, and Gordana Vunjak-Novakovic** From Arteries to Capillaries: Approaches to Engineering Human Vasculature *Adv. Funct. Mater.* 2020, 1910811 © 2020 WILEY-VCH Verlag GmbH & Co. KGaA, Weinheim.

[5] Mattfeldt T, Mall G. Estimation of length and surface of anisotropic capillaries. *Journal of Microscopy.* 1983; 135: 181–190.

[6] Landis EM. Microinjection studies of capillary permeability. II. The relation between capillary pressure and the rate of which fluid passes through the walls of single capillaries. Am J Physiol. 1927; 82(2): 217-238.

[7] Chambers R, Zeweifach BW. Functional activity of the capillary bed with reference to vesciral tissues. *The New York Academy of Sciences* 1946; 46(8): 681-882*.*

[8] Pappenheimer JR, Soto-Rivera A. Effective osmotic pressure of the plasma proteins and other quantities associated with the capillary circulation in the hind limbs of cats and dogs. Am J Physiol. 1948; 152: 471- 491?

[9] Woodcock TE, Woodcock TM. Revised Starling equation and the glycocalyx model of transvascular fluid exchange: an improved paradigm for prescribing intravenous fluid therapy. Br J Anaesth. 2012; 108: 384-394.

[10] Michel CC, Woodcock TE, Curry F-RE. Understanding and extending the Starling principle. Acta Anaesthesiol Scand. 2020; 00: 1–6.

[11] Rhodin JA. The ultra-structure of mammalian arterioles and pre-capillary sphincters. J Ultrastructure Research. 1967; 18: 181–222.

[12] Karnovesky MJ. The ultra-structural basis of capillary permeability studied with peroxidase as a tracer. J Cell Biol. 1967; 35: 213–236. Ivanov KP, Kalinina MK, Levkovich YI. Blood flow velocity in capillaries of brain and muscles and its physiological significance. Microvascular Research. 2020; 22(2): 143-155.

[13] Guyton AC, Coleman TG. Regulation of interstitial fluid volume and pressure. *Annals New York Academy of Sciences.* 1968; 150: 537–547.

[14] Ghanem AN. Magnetic field-like fluid circulation of a porous orifice tube and its relevance to the capillary-interstitial fluid circulation: preliminary report. Med Hypotheses. 2001; 56(3): 325–334.

[15] Ghanem KA, Ghanem AN. The proof and reasons that Starling's law for the capillary-interstitial fluid transfer is wrong, advancing the hydrodynamics of a porous orifice (G) tube as the real mechanism. Blood, Heart and Circ. 2017; 1(1): 17.

[16] Ghanem KA, Ghanem AN. The Physiological Proof that Starling's Law for the Capillary-Interstitial Fluid Transfer is wrong: Advancing the Porous Orifice (G) Tube Phenomenon as Replacement. Open Acc Res Anatomy. 2017; 1(2). OARA.000508.

[17] Ghanem AN. The Correct Replacement for the Wrong Starling's law is the Hydrodynamic of the Porous Orifice (G) Tube: The Complete Physics and physiological Evidence with Clinical Relevance and Significance. Research Article. Cardiology: Open Access Cardio Open. 2020; 5(1): 1-9.

[18] Ghanem AN, Ghanem KA. Revised Starling's Principle (RSP): a misnomer as Starling's law is proved wrong. Med Res Chronicles. 2020.

[19] Ghanem AN. Twenty-one reasons affirming Starling's law on the capillary-interstitial fluid (ISF) transfer wrong and the correct replacement is the hydrodynamic of the porous orifice (G) tube. Case Rep Open A Open J. 2020; I (1): 8-11.

[20] Muhammad Nabeel Syed, Mirza Mujadil Ahmad, Mirza Nubair Ahmad et al. Normal diameter of the ascending aorta in adults: the impact of stricter criteria on selection of subjects free of disease. J Am Coll Cardiol. Mar 2017; 69(11): 2075.

[21] Stücker M, Baier V, Reuther T, Hoffmann, K, Kellam, Keith, Altmey. Capillary Blood Cell Velocity in Human Skin Capillaries Located Perpendicularly to the Skin Surface: Measured by a New Laser Doppler Anemometer. Microvascular research. 1996; 52: 188-92.

[22] Grubb S, Cai C, Hald BO *et al.* Precapillary sphincters maintain perfusion in the cerebral cortex. *Nat Commun.* 2020; 11: 395.

[23] Ishikawa M, Sekizuka E, Shimizu K, Yamaguchi N, Kawase T. Measurement of RBC velocities in the rat pial arteries with an image-intensified high-speed video camera system. Microvascular Research. Nov 1998; 56(3): 166-172.

[24] GUEVARA A-TORRES A, JOSEPH A, SCHALLEK BJ. Label free measurement of retinal blood cell flux, velocity, hematocrit, and capillary width in the living mouse eye. BIOMEDICAL OPTICS EXPRESS. 1 Oct 2016; 7(10): 4235.

[25] Ivanov KP; Kalinina MK; Levkovich YI. Blood flow velocity in capillaries of brain and muscles and its physiological significance. Microvascular Research 2020; 22(2): 143-155.

[26] Hahn RG, Dull RO, Zdolsek J. The Extended Starling principle needs clinical validation. Acta Anaesthesiol Scand. 2020; 64: 884–887.

[27] Ghanem AN. The Adult Respiratory Distress Syndrome: Volumetric Overload Shocks in Patho-Aetiology, Correcting Errors and Misconceptions on Fluid Therapy, Vascular and Capillary Physiology. Surg. Med Open Acc. J. 2(2). SMOAJ.000534.2018.

[28] Ghanem AN. What are Misleading Physicians into giving too much Fluid during Resuscitation of Shock and Surgery that Induces ARDS and/or AKI?" Asploro Journal of Biomedical and Clinical Case Reports. 8 Apr 2020; 3(1): 90-98.

[29] Ghanem AN. Volumetric Overload Shocks (VOS) in Surgical Patients. Open Access J Surg. 2020; 11(2): 555-810.

[30] Ghanem AN. Volume Kinetic Shocks in Clinical Practice. Clin Surg J. 2020; 3(S3): 1-5.

[31] Ghanem AN., Volumetric Overload Shocks Cause the Acute Respiratory Distress Syndrome: The Plenary Evidence on Patho-Aetiology and Therapy. Op Acc J Bio Sci & Res. 2020; 1(4).

[32] Ghanem AN. Volumetric Overload Shocks Cause the Acute Respiratory Distress Syndrome: Building the Bridge Between Physics, Physiology, Biochemistry, and Medicine*.* Biomed J Sci & Tech Res 29(1)-2020. BJSTR. MS.ID.004758.

[33] Ghanem AN. "Volumetric Overload Shocks (VOS) Causing the Acute Respiratory Distress Syndrome (ARDS): The Complete Evidence". EC Emergency Medicine and Critical Care. 2020; 4.2: 01- 08.

[34] Ghanem AN. "Medical World Wake Up, Pay Attention and Listen: Ghanem's New Scientific Discoveries in Medicine, Physiology, Urology, Nephrology, Cardiovascular and Surgery". EC Clinical and Medical Case Reports. 2019; 2.9: 01-06.

[35] Ghanem AN. Editorial. Goodbye Starling's law, hello G tube. J Urol. Nephrol. 2020; 5(1).